

ARTICLE

Open Access



Transmission patterns of multiple strains producing New Delhi metallo- β -lactamase variants among animals and the environment in live poultry markets

Yi Yin¹, Kai Peng¹, Yan Li¹, Wenhui Zhang¹, Yanyun Gao¹, Xinran Sun¹, Sheng Chen³, Zhiqiang Wang^{1,2*} and Ruichao Li^{1,2*} 

Abstract

The widespread transmission of bla_{NDM} among livestock and the live poultry industry attracts considerable public attention. However, studies have not yet addressed its impact on public health in live poultry markets (LPMs). Herein, we investigated the prevalence and genomic epidemiology of bla_{NDM} -positive bacteria in various niches, and explored the transmission patterns of bla_{NDM} within LPMs. Samples were collected between 2019 and 2022 from two LPMs in China. bla_{NDM} was most prevalent in wastewater (35/66, 53.03%). All vegetable samples were negative for bla_{NDM} . bla_{NDM} was mainly distributed among *Escherichia coli* (266/336, 79.17%), *Klebsiella pneumoniae* (62/336, 18.45%), and *Acinetobacter baumannii* (3/336, 0.89%). Some novel hosts, including *Pseudomonas monteilii* and *Pseudomonas otitis*, were also identified. Diverse variants bla_{NDM-1} , bla_{NDM-5} , bla_{NDM-9} , bla_{NDM-13} , and bla_{NDM-27} were identified. The bla_{NDM} -positive *E. coli* ST2659 was dominant. bla_{NDM} was found to coexist with *mcr-1* (4/51, 7.84%). Horizontal gene transfer plays a vital role in bla_{NDM} transmission within the LPMs. Some bla_{NDM} -harboring clones transfer among animals and the environment through the food chain and close contact. More efforts are needed to curb the transmission trend of bla_{NDM} among humans, animals, and the environment within LPMs.

Keywords Live poultry markets, Antibiotic resistance genes, bla_{NDM} , Inter-host transmission

Introduction

According to a recent review published in *The Lancet*, over 1.2 million people died directly from Antimicrobial Resistance (AMR) infections, and an additional 4.95 million deaths were associated with AMR [1]. The emergence of infectious diseases and the spread of AMR severely threaten public health, and hundreds of thousands of people worldwide die from infections caused by multidrug-resistant organisms [2, 3]. Horizontal gene transfer via mobile genetic elements, such as plasmids [4], insertion elements [5], and transposons [6], contributes strongly to the emergence and global spread of multidrug-resistant bacteria [7]. Furthermore, the exchange of antibiotic resistance genes (ARGs) between pathogens

*Correspondence:

Zhiqiang Wang
zqwang@yzu.edu.cn
Ruichao Li
rchl88@yeah.net

¹ Jiangsu Co-Innovation Center for Prevention and Control of Important Animal Infectious Diseases and Zoonoses, College of Veterinary Medicine, Yangzhou University, Yangzhou, Jiangsu, China

² Institute of Comparative Medicine, Yangzhou University, Yangzhou, Jiangsu, China

³ Department of Food Science and Nutrition, Faculty of Science, The Hong Kong Polytechnic University, Kowloon, Hong Kong, China



© The Author(s) 2024. **Open Access** This article is licensed under a Creative Commons Attribution 4.0 International License, which permits use, sharing, adaptation, distribution and reproduction in any medium or format, as long as you give appropriate credit to the original author(s) and the source, provide a link to the Creative Commons licence, and indicate if changes were made. The images or other third party material in this article are included in the article's Creative Commons licence, unless indicated otherwise in a credit line to the material. If material is not included in the article's Creative Commons licence and your intended use is not permitted by statutory regulation or exceeds the permitted use, you will need to obtain permission directly from the copyright holder. To view a copy of this licence, visit <http://creativecommons.org/licenses/by/4.0/>.

and commensal microorganisms from diverse ecological niches increases antibiotic resistance [8]. Over the past decade, numerous studies have investigated the occurrence and spread of ARGs and antibiotic-resistant bacteria in humans, animals, and the environment [9].

Live poultry markets (LPMs), where various live animals are gathered for trading, are highly important for the wholesale and retail of live poultry in China and other Asian countries, and represent a substantial interface between humans, animals, and the environment [10]. LPMs account for about 50% of the live poultry supply to consumers through a complex and non-uniform transportation system, which plays a vital role in live poultry trading [11]. The live animals are imported from different regions and housed at a high density in a relatively compact space alongside other poultry gathered from other places, providing an optimal setting for the transmission and persistence of infectious agents [12]. Hence, LPMs are potential areas where live poultry-associated pathogens, such as some avian influenza viruses, can spread and evolve, causing infection and death in humans [13, 14]. Workers who have been exposed to live poultry for a long term are at a higher risk of contracting avian influenza virus than the consumers [15]. Wang et al. recently showed that LPMs are a huge reservoir of ARGs. Moreover, their diversity here was higher than that in farms, and more abundant ARGs were found in LPM workers than in those who had no contact with LPMs, confirming that live poultry trade promotes the spread of ARGs [16, 17].

Carbapenems, with their broad-spectrum antibacterial activity, are crucial to treat clinical infections in humans caused by multidrug-resistant bacteria. However, overuse and misuse has led to the rapid worldwide proliferation of carbapenem-resistant Gram-negative bacteria [18, 19]. bla_{NDM} represents a typical mobile carbapenem-resistant gene, encoding New Delhi metallo- β -lactamase (NDM), that is often located on plasmids [19]. It encodes a metallo- β -lactamase capable of hydrolyzing most β -lactam antibiotics, particularly meropenem, imipenem, and ertapenem, all three of which are clinically important drugs in the treatment of multidrug-resistant infections. The global prevalence of bacteria carrying bla_{NDM} represents a major public health concern.

bla_{NDM-1} was first detected within *Klebsiella pneumoniae* isolated from a Swedish patient in India in 2008 [20]. Ever since, the number of bla_{NDM} -positive strains isolated from humans, animals, and environment around the world has increased dramatically, posing a major global public health problem [21]. Shen and his team [22] investigated the presence and the genetic environment of bla_{NDM} in slaughterhouses and large-scale livestock and poultry farms in China. Li et al. analyzed the transmission pattern of bla_{NDM} -harboring carbapenem-resistant

E. coli between humans and backyard animals [23]. Li and his colleagues studied the transmission characteristics of bla_{NDM} in the pork production chain [24], while Wang et al. conducted epidemiological research on bla_{NDM} in the live poultry industry chain [25]. However, reports on the distribution and transmission characteristics of bla_{NDM} in LPMs are scarce. Here, we applied a One Health approach to identify the prevalence and transmission mechanism as well as the potential transmission route of bla_{NDM} within various niches in LPMs using a combination of whole-genome sequencing (WGS) and bioinformatic tools.

Results

Prevalence of bla_{NDM} -positive samples in diverse niches

In this study, a total of 593 samples were collected from LPMs A and B in Yangzhou between 2019 and 2022. Of them, 203 samples (336 strains) tested positive for bla_{NDM} , resulting in a positive rate of 34.23% (203/593). The isolation rate of bla_{NDM} -positive samples was higher in LPM B (73/159, 45.91%) compared with LPM A (130/434, 29.95%) (Table S1). Since animals in the LPMs hailed from multiple regions in Jiangsu, a map depicting the sample sources was created (Fig. 1). The isolation rates of bla_{NDM} -positive samples varied across locales. The rates were relatively higher in Huai'an (27/56, 48.21%) and Yancheng (38/89, 42.70%) (Table S3), while Nanjing demonstrated the lowest prevalence rate (2/31, 6.45%). Among the seven areas, Yangzhou contributed the largest number of bla_{NDM} -bearing strains (Fig. 1). In terms of the sources of bla_{NDM} -positive samples, 112 were isolated from chickens (112/312, 35.90%), 18 from ducks (18/30, 46.15%), 7 from pigeons (7/27, 25.93%), 2 from geese (2/17, 11.76%), 1 from soil (1/32, 3.13%), 35 from wastewater (35/66, 53.03%), and 28 from dust (28/87, 34.06%) (Table S4). However, all 13 samples collected from vegetables were bla_{NDM} -negative, and no carbapenem-resistant *E. coli* were recovered. The following species detection rates were found among bla_{NDM} -positive strains: *E. coli* (266/336, 79.17%), *K. pneumoniae* (62/336, 18.45%), and *A. baumannii* (3/336, 0.89%) (Table S5). The five remaining strains included one each of *Acinetobacter bereziniae*, *Enterobacter cloacae*, *Providencia rettgeri*, *Pseudomonas monteilii*, and *Pseudomonas otitidis*.

Antimicrobial susceptibility profiles and resistance and virulence genes

All 336 bla_{NDM} -bearing strains were evaluated for their susceptibility toward a series of β -lactam and non- β -lactam antibiotics (Table S6). Among β -lactam antibiotics, the highest levels of resistance were observed against meropenem (100%), imipenem (100%), ceftiofur (100%),

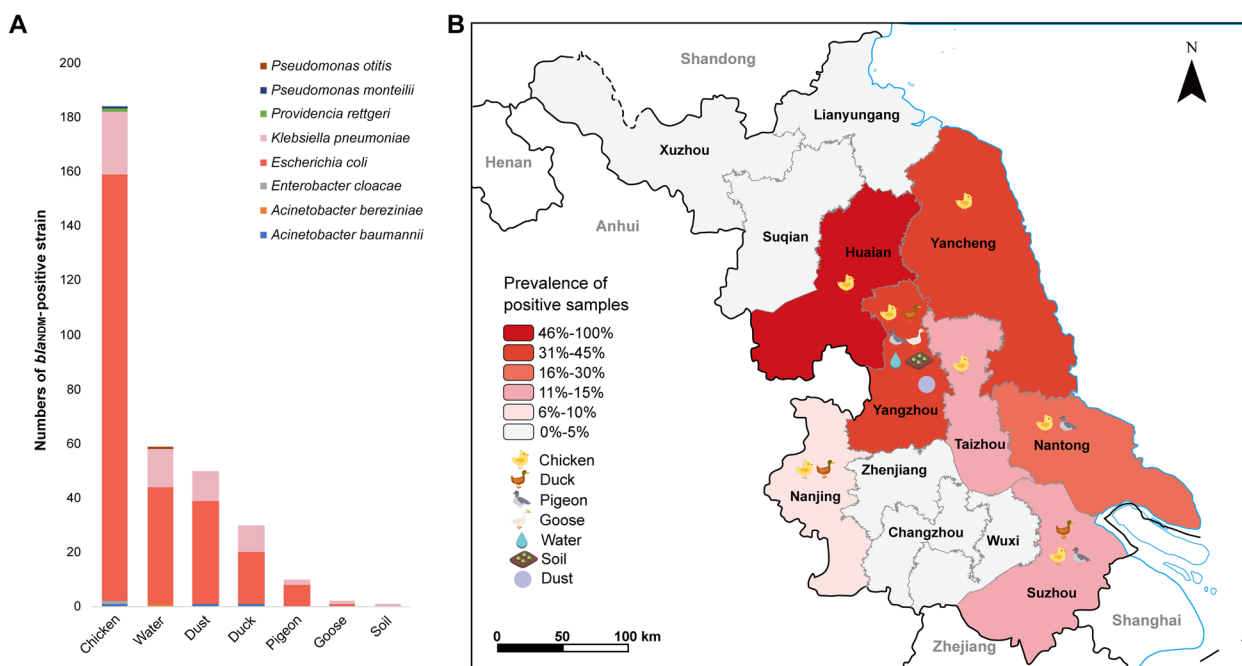


Fig. 1 Prevalence and distribution of *bla*_{NDM}-positive isolates in live poultry markets (LPMs). **A** Distribution of different species of *bla*_{NDM}-positive isolates. **B** Prevalence of *bla*_{NDM}-positive isolates from different regions in Jiangsu province. The prevalence of *bla*_{NDM}-positive samples is marked in red on the map; the darker the color is, the higher the percentage of *bla*_{NDM}-positive samples. The map is based on the standard map GS(2019)3266 without further modifications

and carbenicillin (100%), while >95% of these isolates showed resistance to ampicillin and ceftazidime. Diverse resistance patterns against routinely used non-β-lactam antibiotics were also observed. More than 80% of these isolates were non-susceptible to kanamycin, ciprofloxacin, and gentamicin. Interestingly, *bla*_{NDM}-harboring isolates from animals displayed higher rates of resistance to tigecycline, colistin, kanamycin, and amikacin compared to those from the environment, while the opposite was true regarding resistance to ciprofloxacin (Table S6). The rate of resistance was relatively low to tigecycline (20.53% in animal isolates, 8.33% in environmental isolates) and colistin (7.44% in animal isolates, 2.38% in environmental isolates).

In most instances, the phenotype could be explained by the presence of the appropriate resistance genes. Hence, 51 representative *bla*_{NDM}-harboring isolates were selected and subjected to WGS. These strains were isolated from diverse sources, including different animal feces, wastewater, soil and car surface samples. A total of 77 ARGs were identified, conferring resistance to aminoglycosides, rifampicin, β-lactams, carbapenems, phenicols, macrolides, lincosamides, streptomycin, fosfomicin, colistin, fluoroquinolones, sulfonamides, and tetracyclines, proving that these LPMs were huge reservoirs of ARGs. Among these, *dfra*, which confers resistance to

the veterinary drug trimethoprim/sulfamethoxazole, and *floR*, which confers resistance to florfenicol, were commonly associated with *bla*_{NDM}, with carriage rates of 90.20% (46/51) and 92.16% (47/51), respectively. Compared with other ARGs, the association with *bla*_{NDM} was higher for the spectinomycin resistance gene *aadA* (43/51), the sulfonamide resistance gene *sul2* (37/51), the plasmid-mediated quinolone resistance gene *qnrS1* (29/51), and the tetracycline resistance gene *tet(A)*, which undoubtedly increases the risk of their co-transmission. Notably, the colistin resistance gene *mcr-1* was detected only in four strains, whereas the tigecycline resistance gene *tet(X)* was not identified in any strain, indicating that these isolates might either be inherently resistant or possess other resistance mechanisms. Furthermore, almost half of the *E. coli* isolated from animals and the environment carried multiple virulence genes (*iucABCD*, *iutA*, *iroBCDN* etc.), which serve as good indicators of bacterial pathogenic potentials [1] (Fig. S1).

Comparative susceptibility of *bla*_{NDM}-positive isolates to β-lactam antibiotics

Besides *bla*_{NDM}, other β-lactamase genes, such as *bla*_{OXA-1} and *bla*_{OXA-10}, were detected. Sequence analysis revealed that *bla*_{NDM} from 50 of the 51 isolates differed from *bla*_{NDM-1} by point mutations (Table 1). Among

Table 1 Amino acid substitutions at various positions among NDM variants

NDM variant	Valine 88	Aspartate 95	Glutamate 152	Methionine 154	Alanine 233
NDM-1	-	-	-	-	-
NDM-5	Leucine	-	-	Leucine	-
NDM-9	-	-	Lysine	-	-
NDM-13	-	Asparagine	-	Leucine	-
NDM-27	-	Asparagine	-	-	Valine

the variants, *bla*_{NDM-5}, was the most prevalent, being detected in 42 isolates. *bla*_{NDM-27}, a new variant of NDM that was detected in two isolates of *E. coli* and *K. pneumoniae* from chickens, differed from *bla*_{NDM-1} by amino acid substitutions at positions 95 (Asp→Asn) and 233 (Ala→Val).

To further determine whether the susceptibilities to β-lactam antibiotics were similar for *bla*_{NDM-27} and other variants, we performed conjugation experiments and gene cloning assays. *E. coli* isolates YN1-3, YM3-1, YN23-1, and YN4-1, and *P. rettgeri* YN5-3, which were positive for different *bla*_{NDM} variants (NDM-5, NDM-9, NDM-13, NDM-27, and NDM-1, respectively), were cloned full-length in *E. coli* BL21(DE3), giving rise to BL21(DE3) colonies carrying the recombinant plasmid *bla*_{NDM}. The four *bla*_{NDM} variants from *E. coli* isolates conjugated successfully with *E. coli* C600 as the recipient strain, but *bla*_{NDM-1}

from *P. rettgeri* failed to do so after three attempts, probably due to species differences. We discovered that *bla*_{NDM-27}-positive transconjugants and transformants showed 2–4-fold higher MIC values toward meropenem compared with other *bla*_{NDM} variants (Table 2). Besides, the MIC values of *bla*_{NDM-13}- and *bla*_{NDM-5}-carrying transformants to meropenem were slightly higher than those of *bla*_{NDM-1}- and *bla*_{NDM-9}-carrying transformants. No other variant-specific differences in MIC values were observed toward other β-lactam antibiotics.

Phylogenetic analysis

Given the high isolation rate of *bla*_{NDM}-positive *E. coli* and *K. pneumoniae* in the LPMs as well as their widespread distribution in different animals and environment, 51 representative *bla*_{NDM}-positive strains were chosen for WGS (Table S7). Furthermore, phylogenetic trees were

Table 2 Antimicrobial susceptibility testing of *bla*_{NDM}-positive clinical strains and *E. coli* strains harboring natural and recombinant *bla*_{NDM}-carrying plasmids

Strain	MIC of different β-lactam antibiotics for <i>bla</i> _{NDM} variants (μg/mL)					
	Meropenem	Imipenem	Aztreonam	Ticarcillin	Ceftazidime	Ceftiofur
Original bacteria						
YZLc5-3	256	256	256	512	> 512	> 512
YZLc1-3	> 512	> 512	512	512	> 512	> 512
YZMc3-1	512	512	512	> 152	> 512	> 512
YZLc23-1	> 512	512	256	512	> 512	> 512
YZLc4-1	> 512	> 512	256	> 512	> 512	> 512
Transconjugants						
<i>E. coli</i> C600	≤ 0.125	≤ 0.125	≤ 0.125	4	2	1
C600 + NDM-5	256	128	≤ 0.125	512	256	> 512
C600 + NDM-9	256	256	0.5	> 152	> 512	512
C600 + NDM-13	256	256	1	512	512	> 512
C600 + NDM-27	512	256	1	> 512	512	512
Transformants						
BL21 + pET28a	≤ 0.125	≤ 0.125	≤ 0.125	1	0.5	≤ 0.125
BL21 + pET28a_NDM-1	2	1	0.25	4	4	4
BL21 + pET28a_NDM-5	4	2	≤ 0.125	8	4	4
BL21 + pET28a_NDM-9	2	2	0.25	4	4	8
BL21 + pET28a_NDM-13	4	2	0.5	8	8	8
BL21 + pET28a_NDM-27	8	4	0.5	8	8	8

generated using the *bla*_{NDM}-positive strains from this research and those retrieved from NCBI. We created different phylogenetic trees for the *E. coli* and *K. pneumoniae* variants to analyze the transmission characteristics of *bla*_{NDM} genes in these two species.

Based on core genome SNPs, we built a phylogenetic tree comprising 224 *bla*_{NDM}-positive *E. coli* strains, including 39 from this research and 185 from NCBI (Fig. 2). The isolates retrieved from NCBI came from clinical, animal, and environmental samples from different countries and regions. The 224 *E. coli* strains were divided into eight clades using rhierbaps (<https://rdrr.io/cran/rhierbaps/man/hierBAPS.html>), and the distinctions between the clonal groups were obvious. The 39 *E. coli* strains from this study were assigned to A (11/39, 28.20%), B1 (21/39, 53.85%), D (4/39, 10.26%), E (2/39, 5.13%), and F (1/39, 2.56%), according to Clermont's method (<http://clermontyping.iame-research.center/>),

and these strains were scattered among the eight clonal groups. Overall, the phylogroup determination performed by Clermont's method was generally consistent with the division of clades. Within these strains, *bla*_{NDM-5} was the most prevalent variant (144/224, 64.29%), followed by *bla*_{NDM-1} (27/224, 12.05%) and *bla*_{NDM-9} (23/224, 10.27%). MLST analysis revealed that the 39 *E. coli* strains from this study presented 22 distinct sequence types, with ST2659 (4/39, 10.32%), ST155 (3/59, 5.26%), ST2473 (3/59, 5.26%), and ST162 (3/59, 5.26%) being the most prominent. This is inconsistent with a previous study that reported ST167 and ST101 as the most common *E. coli* sequence types [26]. However, these two sequence types were indeed more prevalent among the *E. coli* strains retrieved from NCBI, with detection rates of 6.48% (12/185) and 3.78% (7/185), respectively. Notably, some same sequence type strains with a low number of SNPs (<150) were found widely distributed in humans,

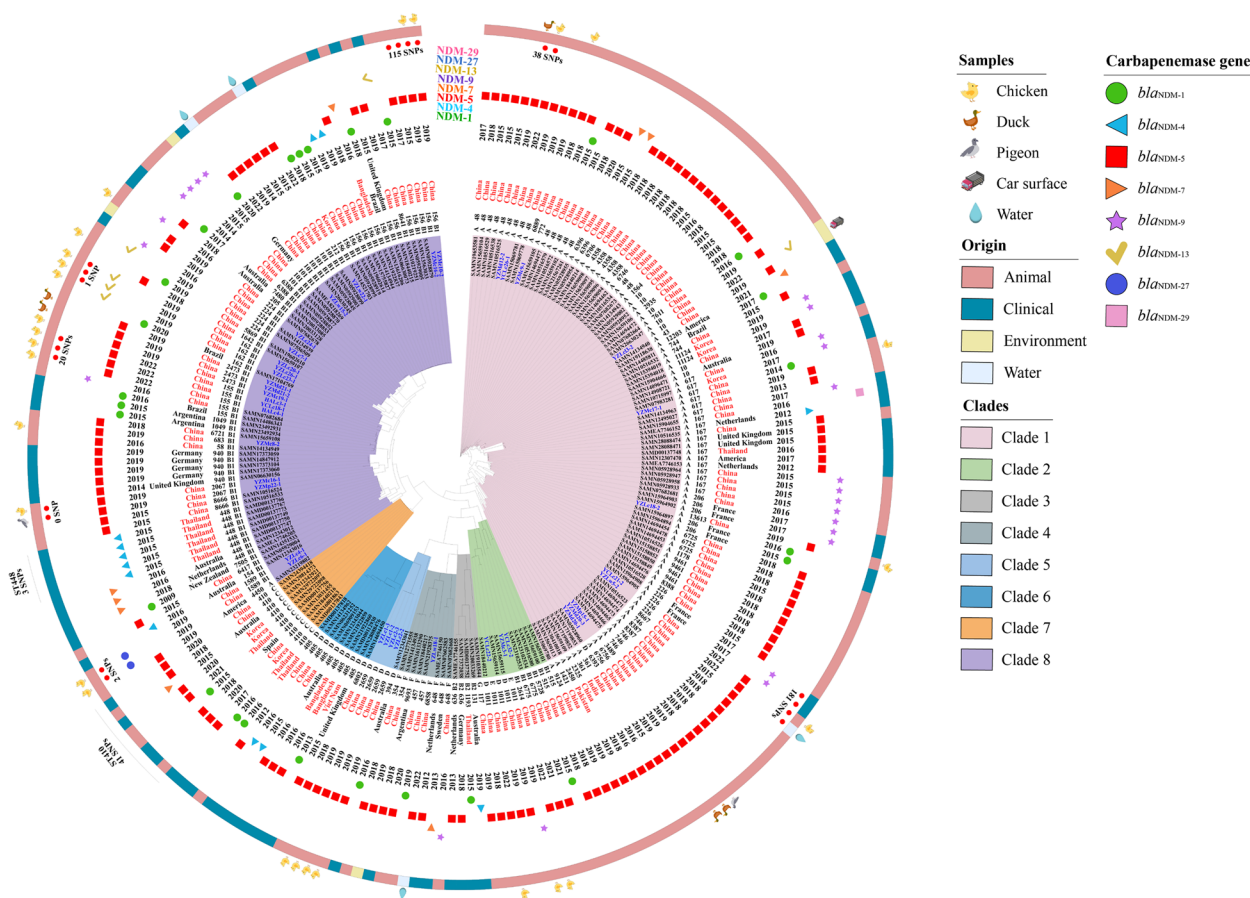


Fig. 2 Phylogenetic analysis of 224 *bla*_{NDM}-positive *E. coli* strains. A phylogenetic maximum-likelihood tree was generated using iTOL software based on single nucleotide polymorphism (SNP) analysis performed using the snp-dists tool (see Table S8 and S9 in the supplemental material). A total of eight clades (pink, green, gray, dark gray, blue, dark blue, orange, and purple) were identified. Strains depicted in dark blue are from this study. Strains positive for *bla*_{NDM-1}, *bla*_{NDM-4}, *bla*_{NDM-5}, *bla*_{NDM-7}, *bla*_{NDM-9}, *bla*_{NDM-13}, *bla*_{NDM-27}, and *bla*_{NDM-29} are indicated by green circles, blue triangles, red squares, pink triangles, purple asterisks, yellow hooks, blue circles, and pink squares, respectively. The origins of *bla*_{NDM}-positive samples in this study are marked outside the outermost circle

animals, and the environment, suggesting that bla_{NDM} genes were probably mediated by the clonal spread of dominant sequence type strains. Furthermore, chicken-derived *E. coli* YCLc26-1 from LPM A displayed 38 SNPs relative to duck-derived *E. coli* YZMd12-2 from the same LPM. The pigeon-derived YZMp22-1 isolate demonstrated no SNPs relative to chicken-derived YZMc16-1, implying that clonal transmission of bla_{NDM} -positive *E. coli* was quite common among various animals in the LPMs. In addition, two bla_{NDM-5} -positive *E. coli* isolates from wastewater and chicken feces were closely related to two bla_{NDM-9} -carrying *E. coli* strains from clinical samples in France. These data further evidence the widespread dissemination of bla_{NDM} across humans and animals worldwide.

For *K. pneumoniae*, we constructed a phylogenetic tree using the 10 isolates from this investigation and 44 bla_{NDM} -positive *K. pneumoniae* strains from NCBI (Fig. S2). The 54 strains were divided into five clades. The clinical samples were mainly concentrated in clades 1 and 2, whereas the animal samples were primarily clustered in clades 4 and 5. The clades could not be discernibly distinguished. Core SNP-based phylogenetic analysis revealed that all isolates from this research shared 157 SNPs and clustered in the same clade, regardless of whether they were isolated from wastewater, chicken feces, soil, or car dust, implying that bla_{NDM} -positive *K. pneumoniae* not only transmitted clonally between animals and the environment in the LPMs, but could also disseminate through vehicles. Moreover, all these strains belonged to the same sequence type, ST5241, and harbored highly identical plasmid replicons, ARGs, and virulence genes, suggesting that *K. pneumoniae* ST5241 could be present in various niches in the LPMs. Hence, effective strategies must be devised to reduce the prevalence and dissemination of this *K. pneumoniae* strain.

Transmissibility and characteristics of bla_{NDM} -harboring plasmids

Plasmids carrying bla_{NDM} from 225 strains were successfully transferred into *E. coli* C600 or *E. coli* J53. The conjugation frequency of the transconjugants ranged from 10^9 – 10^2 (Table S6). Among all the plasmid replicon types tested in this study, the highest conjugation frequency of 10^6 – 10^4 was exhibited by IncX3-type plasmids (Table S12).

To further investigate the genetic background of bla_{NDM} -bearing bacteria and its role in dissemination, seven strains carrying different bla_{NDM} variants from various clades in the phylogenetic tree were completely sequenced to reveal plasmid characteristics (Table S7). The expression of all seven bla_{NDM} genes was

mediated by plasmids, but these genes did not coexist with *mcr-1* (Fig. 3). Three almost distinct transmissible bla_{NDM-5} -bearing plasmids from chicken-derived *E. coli* strains YZMc10-2, YZMc17-1, and YZLc1-3 were detected, with sizes ranging from 46–245 kb. Replicon analysis revealed that these plasmids belonged to different Inc types, including IncHI2-HI2A, IncFII, and IncX3, respectively. pYZMc10-2_NDM-5_245k, with the most abundant resistance genes and the highest conjugation frequency, shared over 99% identity and 100% coverage with a chicken-derived bla_{NDM-5} -positive plasmid isolated in 2020 (MT407547), indicating the potential long-term occurrence of IncHI2-HI2A bla_{NDM-5} -positive plasmids (Fig. 3A). In addition, pYZMc3-1_NDM-9_226k shared relatively low coverage rates of 67% and 13% with bla_{NDM-9} -positive plasmids within *Salmonella enteritidis* from chickens and *E. coli* from retail meat, respectively. However, all three bla_{NDM-9} positive plasmids harbored a multidrug-resistant region of approximately 9 kb, containing multiple mobile genetic elements, which could be transferred and integrated into other plasmids via circular intermediates (Fig. 3B). pYZLc4-1_NDM-27_46k, which is 46,283 bp long and carries the bla_{NDM-27} variant, has never been reported previously. This bla_{NDM-27} -carrying plasmid was successfully transferred into *E. coli* C600, and the conjugation frequency was 4.47×10^{-6} . It belongs to the IncX3 plasmid type, which is the most common plasmid type worldwide [5]. The bla_{NDM} -positive plasmids that were isolated from Vietnamese chickens (LC570846), Chinese chickens (MH286946), and Chinese ducks (MK628734), and retrieved from NCBI shared up to 100% homology with pYZLc4-1_NDM-27_46k, indicating that IncX3-type bla_{NDM} -positive plasmids are relatively conserved in different ecological niches (Fig. 3C). The backbone of the bla_{NDM-13} -carrying plasmid was relatively simple, and showed 85% coverage and 99.88% homology with p1_020022 isolated from a clinical sample in Sichuan (CP032880). The two plasmids differed only in their multi-drug resistance region, indicating that this region in the bla_{NDM-13} -carrying plasmid was mobile and could be mediated by the insertion sequence to spread among different *Enterobacteriaceae* species (Fig. 3D). Notably, the non-transferable pYZLc5-3_NDM-1_129k plasmid possessed a plasmid-free replicon similar to the plasmid backbone of bla_{NDM} -negative strains that were isolated from Nantong pig farms (CP047346) and Shandong chicken farms (CP073357) in 2018. Further analysis revealed that the two bla_{NDM-1} -negative bacteria lacked the conserved structure of bla_{NDM-1} -*ble*_{MBL}-*trpF*-*tat* mediated by IS*Aba125*, highlighting the significant role of the

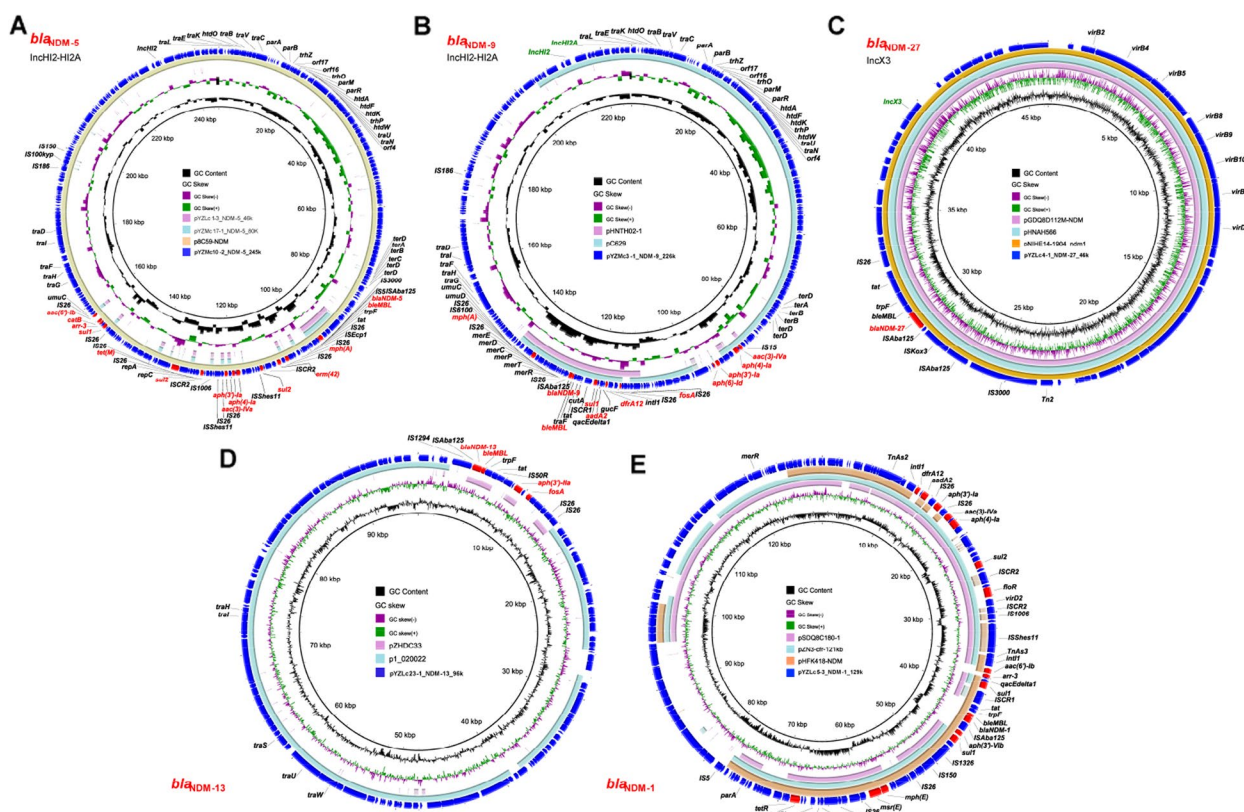


Fig. 3 The genetic environment of *bla*_{NDM}-positive plasmids. The GC skew and GC content are indicated from the inside out. The arrows represent the positions and transcriptional directions of the open reading frames (ORFs). Genes are differentiated by color. **A, B, C, D, E,** and **F** represent different *bla*_{NDM}-bearing plasmids with different *bla*_{NDM} variants (*bla*_{NDM-5}, *bla*_{NDM-9}, *bla*_{NDM-27}, *bla*_{NDM-13}, and *bla*_{NDM-1})

insertion sequence in mediating the transfer of ARGs (Fig. 3E).

The diversity of *bla*_{NDM} variant-bearing genetic contexts

To further analyze the transmission mechanism of *bla*_{NDM}-harboring plasmids, we conducted a comprehensive analysis of the core genetic environment of 51 *bla*_{NDM}-positive strains that were subjected to sequencing. The region downstream of *bla*_{NDM}, *bla*_{NDM}-*ble*_{MBL}-*trpF*-*tat*, is fairly conserved (Fig. 4). Based on sequence homology, we categorized the core genetic environment into six types: G1 (1/51), G2 (1/51), G3 (5/51), G4 (2/51), G5 (28/51), and G6 (14/51).

The G1 type was flanked by two inverted IS26 elements, and the upstream 10,473-bp region shared high homology with the region found in *S. enteritidis* C629 (CP015725) (Fig. 3B), encompassing 13 genes from the truncated *IS**Aba125* to *intl1*. Moreover, the G1 type harbored a multidrug resistance region, *sul1*- Δ *qacE-hp*-*aadA2*-*dfrA12*, between *ISCR1* and *intl1*, conferring resistance to sulfonamides, aminoglycosides, and trimethoprim. On the other hand, the G2 type, with an 18,625-bp-long backbone, carried the cassette

*IS**Aba125*-*bla*_{NDM}-*ble*_{MBL}-*trpF*- Δ *tat*-*ISCR1*-*sul1*- Δ *qacE-hp*-*arr-3*, which was also found in the *bla*_{NDM-1}-positive plasmid pHFk418-NDM from *Proteus mirabilis* (MH491967) (Fig. 3D), along with the truncated transposons TnAs3 and *ISShes11* downstream. The G3 type, which was associated with five *bla*_{NDM-13}-positive strains isolated from chicken feces and car dust, was characterized by the presence of *IS1294* upstream of *bla*_{NDM-13}, the absence of *ISCR1* downstream, and the presence of truncated *IS50R* and *IS26*. Both the G4 and G5 genetic contexts contained *IS3000* and *IS26*, and *bla*_{NDM-5} could be integrated into the *E. coli* plasmid through an *IS3000*-mediated replicative transposon [27]. *IS26* has also been implicated in capturing and mobilizing the transfer of *bla*_{NDM} in *Enterobacter* species [28], indicating that insert sequences may play a vital role in the transmission of ARGs. However, while the G4 type was characterized by the presence of *ISKox3* upstream of *bla*_{NDM}, the G5 type included *IS5* upstream of *bla*_{NDM}. The G5 type served as the predominant genetic environment of the widely prevalent *bla*_{NDM-5}-positive plasmids in the LPMs. These plasmids have been detected in diverse sample sources, including various animals and environments.

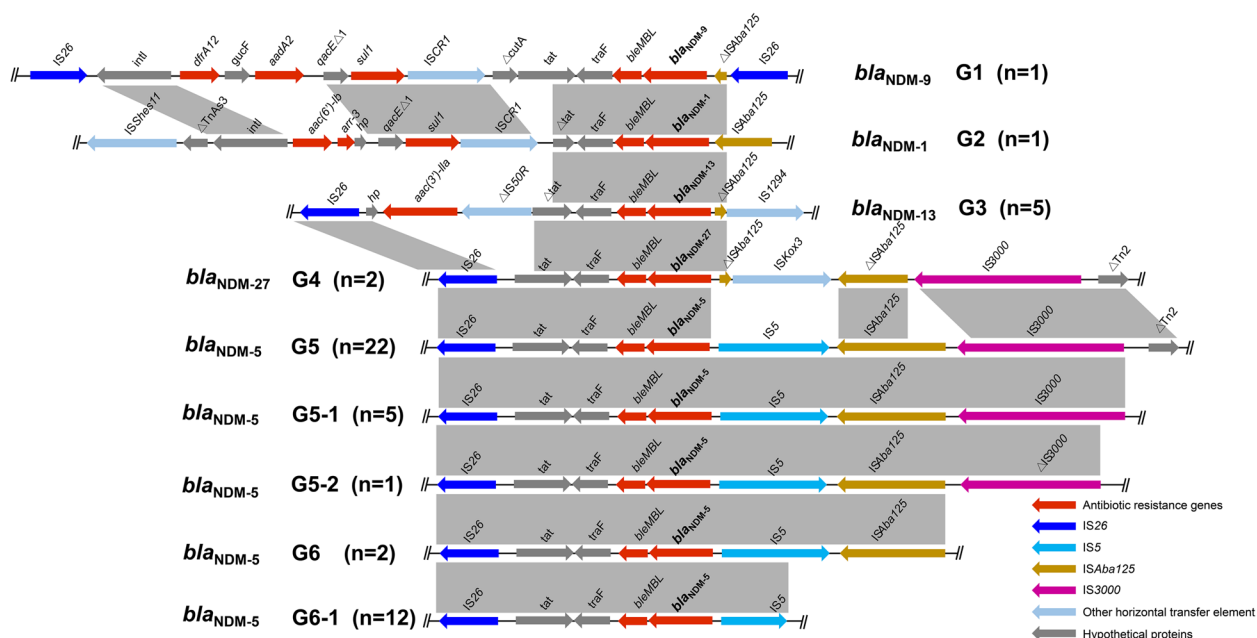


Fig. 4 Different types of genetic environments of various *bla*_{NDM} genes. Major types of *bla*_{NDM}-carrying genetic contexts among the 51 *bla*_{NDM}-bearing plasmids

Notably, the core genetic environment of the *bla*_{NDM-5}-positive plasmid isolated from the LPMs shares 100% homology with that of the *bla*_{NDM-5}-positive plasmid found in carbapenem-resistant *Enterobacteriaceae* isolated from humans in China [29], suggesting that the G5-type genetic environment, with the help of insertion sequences such as IS26 and IS3000, has been widely disseminated across different ecological niches in the LPMs. Furthermore, subtypes G5-1 and G5-2 were identified based on the integrity of IS3000 upstream of *bla*_{NDM-5} and the presence of the truncated transposon Tn2. In contrast, IS3000 is absent upstream of *bla*_{NDM-5} in the G6 type, while the G6-1 subtype also lacks ISAbal125.

We used a Sankey diagram to elucidate the relationships between the *bla*_{NDM} core genetic environment and various factors, such as species, strain source, plasmid replicon type, and *bla*_{NDM} variant (Fig. 5). G5 exhibited the highest prevalence (28/51, 54.9%), followed by G6 (14/51, 27.45%). It is worth noting that *E. coli* exhibits a greater diversity of *bla*_{NDM} bearing genetic contexts than the more homogeneous genetic context G6-1 observed in *K. pneumoniae*. Interestingly, IncHI2-HI2A plasmids were more prevalent (27/51) than IncX3 plasmids (13/51) in this study, whereas previous studies have reported the opposite trend in China [5]. This discrepancy might be attributed to the concentration and limitations of the sampling area. The presence of six other *bla*_{NDM}-positive plasmid replicons in the environment indicated the ubiquitous nature of *bla*_{NDM} in *Enterobacteriaceae*.

Discussion

Over the past decade, *bla*_{NDM}-positive strains have been increasingly isolated from humans [30, 31], animals [21], and the environment [32] worldwide, raising global concern in the field of public health. LPMs represent a key human–animal interface because live animals from various areas are congregated here for trade in urban areas. However, the prevalence and transmission mechanisms of *bla*_{NDM} in different ecological niches within LPMs have rarely been studied [17, 33, 34]. Therefore, the rapid spread of *bla*_{NDM}-harboring strains in LPMs has not yet been considered a major threat to public health yet.

For the first time here, using a One Health approach, we have provided evidence of the potential transmission of *bla*_{NDM}-positive bacteria through the food chain or through close contact between different animals and their environment in LPMs. The key findings of this study are as follows: (a) Over 65% of *bla*_{NDM} genes were able to be transferred, including cross-species transmission, and the conjugative transfer frequency was concentrated at 10⁻⁵, suggesting that *bla*_{NDM} has been extensively disseminated throughout the LPMs; (b) Some *bla*_{NDM}-harboring strains isolated from chickens, ducks, pigeons, and car dust showed similar genotypes based on SNP analysis, suggesting that different niches within LPMs could serve as an important transmission medium for *bla*_{NDM}-positive strains, facilitating the spread of ARGs across different ecological niches; (c) The *bla*_{NDM} core genetic environment G5 was detected

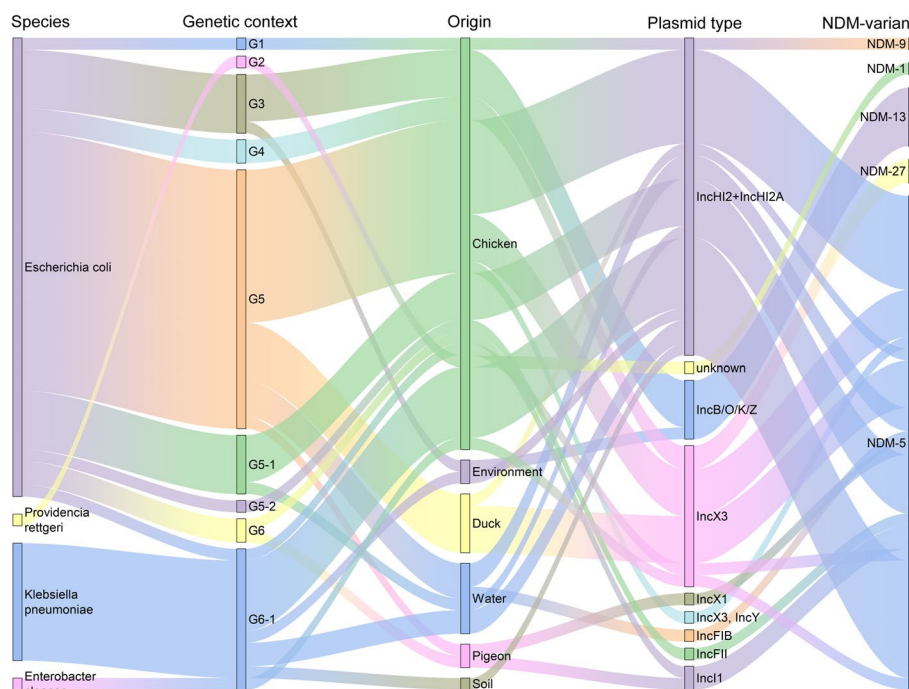


Fig. 5 Sankey diagram combining the species, genetic environment, source of strains, plasmid replication types, and *bla*_{NDM} variants. The diameter of the line is proportional to the number of isolates, which are also labeled at the consolidation points

with 100% homology in 43% of the strains, isolated from various animal and environmental samples; and d) Over 20% of the strains isolated from animal samples shared the same sequence type as that of strains isolated from environmental samples, further corroborating the possibility that the different niches can act as a transmission medium. The above results indicate the possibility of clonal transmission among animals and the environment in LPMs through the food chain and close contact. Based on these findings, we concluded that LPMs are an underestimated hotspot for the spread of multidrug-resistant bacteria among animals and the environment. This conclusion underscores the critical role played by LPMs in the dissemination and evolution of drug-resistant bacteria, and highlights the need for enhancing regulatory and control measures in these niches to curb the emergence and spread of ARGs. Furthermore, these findings call for stricter monitoring of animals and the environment in LPMs to promptly detect and control potential pathogen transmission risks, ensuring the health and safety of humans and animals.

Five *bla*_{NDM} variants, including *bla*_{NDM-27}, a newly reported variant, were isolated from the LPMs. We found that the MIC values of *bla*_{NDM-27}-positive transconjugants to meropenem were 2–4-fold higher than those of isolates carrying other variants. Amino acid substitutions were found at positions 95 and 233, with Asp being

replaced by Asn and Ala by Val, respectively. Previous studies have shown that substitutions at these positions can affect enzyme kinetics and drug resistance; for example, NDM-3, which has an amino acid substitution at position 95, showed a slightly lower k_{cat}/K_m ratio compared with NDM-1 [35]. NDM-6, which has an amino acid substitution at position 233, exhibited higher drug resistance than NDM-1, particularly against meropenem and imipenem [36]. However, it had lower thermal stability than NDM-1 [37]. Therefore, substitutions at positions 95 and 233 might enhance drug resistance of *bla*_{NDM}-positive strains, while compromising on their environmental stability. Further research is needed to explore whether these substitutions affect enzyme activity and thermal stability. The *bla*_{NDM} variants detected in this study were distributed among various species as previously reported [38], with *E. coli* being the most common. These species were isolated from various animal and environmental samples. More than half of the wastewater samples contained *bla*_{NDM} (35/66). This water is primarily used as drinking water for animals and domestic water for workers, increasing the risk of *bla*_{NDM} transmission to humans and animals in the LPMs. The tetracycline resistance genes *tet(X3)* and *tet(X4)* have been previously detected in the workers and environment of LPMs [17], hinting at their transmission from animals to humans and the environment via plasmids, corroborating

the notion of LPMs being potential reservoirs of ARGs. All niches within LPMs are at risk of supporting the dissemination of *bla_{NDM}*, emphasizing the need to adopt a One Health approach to prevent the transmission of pathogenic bacteria.

Although we provide evidence of the transfer of *bla_{NDM}*-positive strains between animals and the environment in LPMs, we acknowledge several limitations in this study. First, a large sample size of LPM workers was unable to be used in the present study due to sampling limitations associated with the large workload and high cost. However, phylogenetic analysis has shown that *bla_{NDM}*-positive strains are widespread among humans, animals, and the environment globally. Previous research has also indicated that workers with prolonged exposure to LPM environments may harbor a higher abundance of ARGs than workers in a control group. Therefore, we hypothesized that LPM workers could carry and spread *bla_{NDM}*-positive isolates through close contact or the food chain (Fig. 6). Second, considering the significant differences in the number of different animals in LPMs, it is worth noting that chickens account for up to 80% of the total number of LPMs. This disparity can largely be attributed to the eating habits prevalent in our country. To provide a more accurate reflection of the market situation, our sample collection process focused primarily on chickens. Of the 395 samples collected, 312 were derived from chicken manure, accounting for approximately 78.99% of the total samples. However, it is important to acknowledge that this sampling strategy may introduce some bias in the sample size. Furthermore, although we collected 593 samples from various ecological niches in

LPMs, it is important to note that the sampling was primarily focused on two LPMs. As a result, the findings may not entirely represent the overall prevalence and transmission mechanism of *bla_{NDM}*-positive bacteria in LPMs. Therefore, it is crucial to broaden our sampling scope and include more LPMs in our study. By adopting this comprehensive sampling strategy, we can gain a more comprehensive understanding of the transmission pathways of *bla_{NDM}*-positive strains in this environment. By considering the actual situation, we can develop and implement appropriate measures to effectively mitigate the spread of *bla_{NDM}*-positive strains in LPMs [39].

Conclusion

To our knowledge, this is the first and most comprehensive surveillance of *bla_{NDM}*-positive bacteria in humans, animals, and environmental niches within LPMs. These bacteria were more prevalent among wastewater, ducks, chickens, and dust samples, and less prevalent among pigeons, geese, and soil samples. *bla_{NDM}* genes were distributed between two main species, *E. coli* and *K. pneumoniae*. *bla_{NDM}*-carrying bacteria were highly diverse and frequently associated with multidrug resistance phenotypes. Horizontal gene transfer mediated by the IncHI2-HI2A plasmid and the core genetic environment G5 formed the major transmission mechanism of *bla_{NDM}* within the LPMs. Phylogenetic analysis evidenced the transmission of *bla_{NDM}*-harboring bacteria between animals and the environment, and suggested that humans might play a crucial role in this transmission via the food chain and close contact.

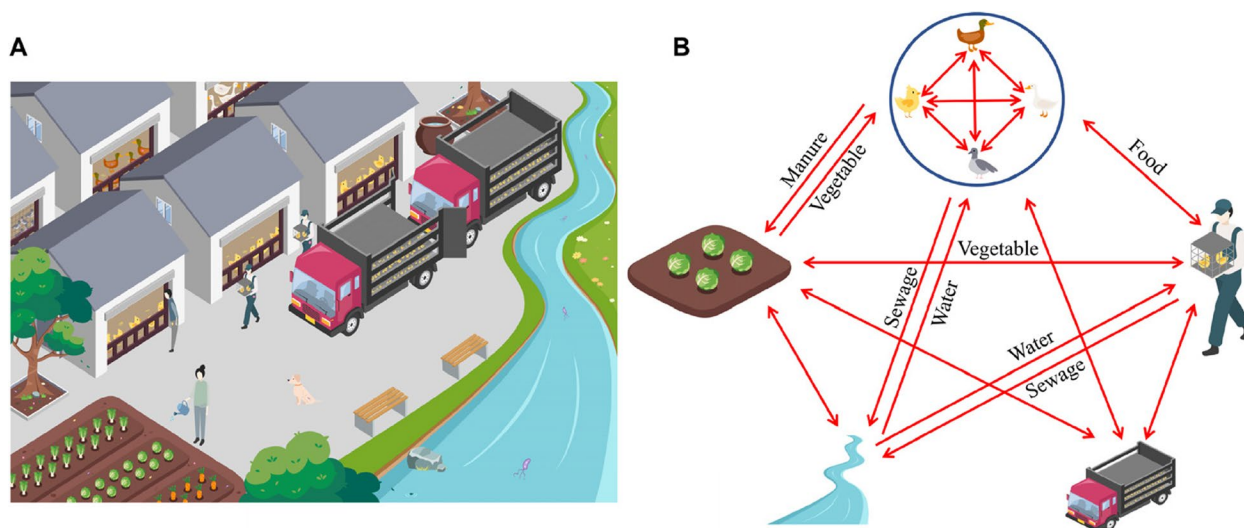


Fig. 6 Diagram showing possible transmission routes for *bla_{NDM}*-positive strains among humans, animals, and the surrounding environment in LPMs. **A** The production mode of LPMs. **B** Possible transmission routes of *bla_{NDM}*-positive strains

Materials and methods

Sample collection and screening of *bla*_{NDM}-positive strains

Samples were collected between April 1, 2019 and July 31, 2022, from two large-scale LPMs in Yangzhou to investigate the epidemiology of *bla*_{NDM}-positive bacteria in animals and the environment (Table S2). The animals gathered in the LPMs were from different regions (Huai'an, Yancheng, Yangzhou, Taizhou, Nanjing, Nantong, and Suzhou) of the Jiangsu Province (Fig. 1, Table S3). A total of 593 non-duplicate samples were collected, comprising animal feces (chicken, $n=312$; duck, $n=39$; pigeon, $n=27$; goose, $n=17$) and environmental samples (soil, $n=32$; wastewater, $n=66$; vegetables, $n=13$; dust, $n=87$) (Table S4). Sterilized water was used as a transfer medium for the dust samples. All the samples were kept in cool boxes with ice packs (4 °C) while being transported to the laboratory for bacterial cultivation and DNA extraction.

Samples were spread onto MacConkey plates supplemented with 2 mg/L meropenem, and incubated for 18 h at 37 °C. Different colored colonies were selected from each plate for identifying carbapenem-resistant isolates. Cultures were identified using MALDI-TOF MS AximaTM [40] and 16S rRNA gene sequencing (Table S1). All confirmed carbapenem-resistant strains were investigated for the presence of *bla*_{NDM} genes (Table S1).

Antimicrobial susceptibility testing

Antimicrobial susceptibility was tested using the broth dilution method. The susceptibility of carbapenem-resistant isolates was tested for antimicrobial drugs commonly used in both medical and veterinary settings, including meropenem, imipenem, ampicillin, ceftazidime, tigecycline, kanamycin, amikacin, ciprofloxacin, gentamicin, colistin, ceftiofur, and carbenicillin. Minimum inhibitory concentrations (MICs) were interpreted according to the guidelines provided by the Clinical and Laboratory Standards Institute (2021) [41], along with the breakpoint tables specified in version 12.0 of the European Committee on Antimicrobial Susceptibility Testing. As a control, we employed *E. coli* American Type Culture Collection 25922 as a quality control measure.

Plasmid conjugation assay

To investigate the transferability of *bla*_{NDM}-bearing genetic elements, we utilized rifampicin-resistant *E. coli* C600 and sodium azide-resistant *E. coli* J53 as the recipients for the conjugation assay. The liquid mating method was employed for this experiment. To begin with, overnight cultures of the original isolates and recipient strains were grown in Luria-Bertani (LB) broth. The cultures were then adjusted to an optical density of 0.6 at 600 nm.

A 5- μ L portion of each culture was diluted 1:200 in fresh LB broth and incubated at 37 °C with gentle shaking for a period of 4 h. Subsequently, the conjugation mixtures were diluted tenfold and plated on selective agar plates to quantify the recipients (rifampicin/sodium azide) as well as the transconjugants (rifampicin plus meropenem/sodium azide plus meropenem). The conjugation frequency was determined by calculating the ratio of transconjugants obtained per input recipient cell [42]. Finally, PCR analysis was carried out to conclusively verify that the transconjugants were indeed derived from the recipient *E. coli* strains C600 and J53.

WGS of the flanking region of *bla*_{NDM}

We utilized the FastPure Bacteria DNA Isolation Mini Kit (Vazyme, Nanjing, China) to extract the genomes of 51 strains resistant to meropenem. The extracted DNA's concentration and purity underwent assessment through NanoDrop 2000 and gel electrophoresis, with final precise concentration confirmation using the QubitTM 4.0 fluorometer (Invitrogen, CA, USA). Subsequently, Illumina HiSeq 2500 was employed for short-read sequencing of the extracted DNA, generating paired-end reads measuring 2 \times 150-bp. Following this, we subjected the collected raw reads, with a minimum coverage of 100-fold, to trimming using Trimmomatic v.0.36 [43]. De novo assembly was then conducted using SPAdes v.3.13.1 [44]. Based on diverse resistant phenotypes and phylogenetic analysis, we identified seven representative strains for further sequencing using Nanopore MinION [45], which provided single-molecule long reads. We achieved the complete genome by employing hybrid assembly of both short and long reads via Unicycler v.0.4.8 [46]. The putative coding sequences flanking the *bla*_{NDM} genes were annotated by Rapid Annotations using Subsystems Technology (<https://rast.nmpdr.org/>). To analyze the plasmid type, ARGs, virulence genes, and mobile genetic elements of the *bla*_{NDM}-positive isolates, we utilized ABRicate (<https://github.com/tseemann/abricate>). Additionally, we generated a circular genome comparison map using BLAST Ring Image Generator [47] while EasyFig [48] was implemented for the line alignment of core genetic structures.

Phylogenetic analysis of *bla*_{NDM}-bearing isolates from various origins

The assembled genomes of *bla*_{NDM}-positive strains, with complete isolation information, were retrieved and then downloaded from the National Center for Biotechnology Information (NCBI; as of 1 September, 2022) (<https://www.ncbi.nlm.nih.gov/pathogens>). Draft genome sequences were re-annotated using Prokka v.1.11 [49], and core genomes were extracted and aligned using

Roary v.3.6.1 [50] before being subjected to phylogenetic tree construction using FastTree v.1.4.3 [51]. The phylogenetic tree was visualized and embellished with the corresponding features of each isolate using iTOL (<https://itol.embl.de/>), and multilocus sequence typing (MLST) was performed according to PubMLST (<https://pubmlst.org/>). To estimate the phylogenetic groups (A, B1, B2, D, E, and F) of the *E. coli* isolates, the assembled genome was uploaded to ClermonTyping based on the concept of in vitro PCR assays [52]. Single nucleotide polymorphisms (SNPs) were analyzed using snp-dists v.0.7.0 to detect pairwise SNP distances. Resistance genes and virulence genes were visualized using TBtools [53]. WGS data generated from this study have been deposited in GenBank and under BioProject accession no. PRJNA877800.

Comparative susceptibility analysis of different *bla*_{NDM} variants to β -lactam antibiotics

To assess and compare the susceptibility of different *bla*_{NDM} variants to different β -lactam antibiotics, 849-bp-long DNA fragments comprising the complete *bla*_{NDM} gene and homology arm were amplified using primers (Table S1), ligated into pET-28a(+) using ClonExpress II One Step Cloning Kit (Vazyme, Nanjing, China), and expressed in *E. coli* BL21(DE3). Transformants were selected on LB agar plates containing 2 mg/L meropenem and 100 mg/L kanamycin, and confirmed by Sanger sequencing with T7 primer (Table S1). Antimicrobial susceptibility was tested using different β -lactam antibiotics (meropenem, imipenem, aztreonam, ticarcillin, ceftazidime, and ceftiofur) on transconjugants and transformants to compare the susceptibilities of different *bla*_{NDM} variants [36].

Supplementary Information

The online version contains supplementary material available at <https://doi.org/10.1186/s44280-024-00050-2>.

Additional file 1: Table S1. Primers used in this study. **Table S2.** The prevalence of *bla*_{NDM}-positive samples in LPMs A and B. **Table S3.** Number of *bla*_{NDM}-positive samples from LPMs and their prevalence among different regions in Jiangsu. **Table S4.** Origins and numbers of *bla*_{NDM}-positive strains in LPMs. **Table S5.** Species and numbers of *bla*_{NDM}-positive strains in LPMs. **Table S6.** Antibiotic susceptibility testing (MICs, mg/L) of 336 *bla*_{NDM}-positive strains. **Table S7.** Basic information of 51 *bla*_{NDM}-positive strains sequenced by Illumina/Nanopore sequencing. **Table S8.** Basic information of *bla*_{NDM}-positive strains used for phylogenetic analysis in Fig. 2. **Table S9.** The SNPs distribution of *bla*_{NDM}-positive strains used for phylogenetic analysis in Fig. 2. **Table S10.** Basic information of *bla*_{NDM}-positive strains used for phylogenetic analysis in Fig. 3. **Table S11.** The SNPs distribution of *bla*_{NDM}-positive strains used for phylogenetic analysis in Figure S2. **Table S12.** Characteristic of *bla*_{NDM}-bearing plasmids in different bacterial species from LPMs. **Fig. S1.** The heat map of resistance genes and virulence genes of 51 *bla*_{NDM}-positive isolates in this study. The darker the blue, the higher the similarity. **Fig. S2.** Phylogenetic analysis for 54 *bla*_{NDM}-positive *K. pneumoniae* strains. Phylogenetic maximum-likelihood

tree generated using iTOL software based of SNP analysis performed using the snp-dists tool (see Table S10 and S11 in the supplemental material). A total of five clades (green, blue, purple, yellow, and pink) were identified. Strains expressed by red are from this study.

Authors' contributions

Y.Y.: Conceptualization, Data curation, Formal analysis, Investigation, Methodology, Software, Visualization, Writing – original draft. K.P.: Conceptualization, Writing – review & editing. Y.L.: Writing – review & editing. W.Z.: Writing – review & editing. Y.G.: Sample collection, Writing – review & editing. X.S.: Sample collection, Writing – review & editing. S.C.: Supervision, Writing – review & editing. Z.W.: Supervise this project equally, Writing – review & editing. R.L.: Supervision, Project administration, Writing – review & editing.

Funding

This work was supported by the Sichuan Science and Technology Program (2022ZDZX0017), the National Natural Science Foundation of China (32161133005), the China Postdoctoral Science Foundation (2022T150555) and the Priority Academic Program Development of Jiangsu Higher Education Institutions (PAPD).

Availability of data and materials

WGS data generated from this study have been deposited in GenBank and under BioProject accession no. PRJNA877800.

Declarations

Ethics approval and consent to participate

Not applicable.

Consent for publication

Not applicable.

Competing interests

The authors declare that they have no competing interest.

Received: 29 December 2023 Revised: 25 March 2024 Accepted: 16 April 2024

Published online: 09 May 2024

References

1. Antimicrobial Resistance Collaborators. Global burden of bacterial antimicrobial resistance in 2019: a systematic analysis. *Lancet*. 2022;399:629–55.
2. He T, Wang R, Liu D, Walsh TR, Zhang R, Lv Y, et al. Emergence of plasmid-mediated high-level tigecycline resistance genes in animals and humans. *Nat Microbiol*. 2019;4:1450–6.
3. Liu L, Su J, Guo Y, Wilkinson DM, Liu Z, Zhu Y, et al. Large-scale biogeographical patterns of bacterial antibiotic resistance in the waterbodies of China. *Environ Int*. 2018;117:292–9.
4. Rodríguez-Beltrán J, DelaFuente J, León-Sampedro R, MacLean RC, San Millán Á. Beyond horizontal gene transfer: the role of plasmids in bacterial evolution. *Nat Rev Microbiol*. 2021;19:347–59.
5. Acman M, Wang R, van Dorp L, Shaw LP, Wang Q, Luhmann N, et al. Role of mobile genetic elements in the global dissemination of the carbapenem resistance gene *bla*_{NDM}. *Nat Commun*. 2022;13:1131.
6. Rinkel M, Hubert JC, Roux B, Lett MC. Identification of a new transposon Tn5403 in a *Klebsiella pneumoniae* strain isolated from a polluted aquatic environment. *Curr Microbiol*. 1994;29:249–54.
7. Carattoli A. Plasmids and the spread of resistance. *Int J Med Microbiol*. 2013;303:298–304.
8. Bengtsson-Palme J, Larsson DGJ. Antibiotic resistance genes in the environment: prioritizing risks. *Nat Rev Microbiol*. 2015;13:396–396.
9. Morehead MS, Scarbrough C. Emergence of global antibiotic resistance. *Prim Care*. 2018;45:467–84.
10. Gao X, Shao M, Luo Y, Dong Y, Ouyang F, Dong W, et al. Airborne bacterial contaminations in typical Chinese wet market with live poultry trade. *Sci Total Environ*. 2016;572:681–7.

11. Lei X, Jing S, Zeng X, Lin Y, Li X, Xing Q, et al. Knowledge, attitudes and practices towards avian influenza among live poultry market workers in Chongqing, China. *Prev Vet Med.* 2019;162:151–9.
12. Li B, Ma L, Li Y, Jia H, Wei J, Shao D, et al. Antimicrobial resistance of *Campylobacter* species isolated from broilers in live bird markets in Shanghai, China. *Foodborne Pathog Dis.* 2017;14:96–102.
13. Yuan J, Lau EH, Li K, Leung YH, Yang Z, Xie C, et al. Effect of live poultry market closure on avian influenza A(H7N9) virus activity in Guangzhou, China, 2014. *Emerg Infect Dis.* 2015;21:1784–93.
14. Zhou L, Liao Q, Dong L, Huai Y, Bai T, Xiang N, et al. Risk factors for human illness with avian influenza A (H5N1) virus infection in China. *J Infect Dis.* 2009;199:1726–34.
15. Chen Y, Cheng J, Xu Z, Hu W, Lu J. Live poultry market closure and avian influenza A (H7N9) infection in cities of China, 2013–2017: an ecological study. *BMC Infect Dis.* 2020;20:369.
16. Wang M, Zhang R, Wang L, Sun R, Bai S, Han L, et al. Molecular epidemiology of carbapenemase-producing *Escherichia coli* from duck farms in south-east coastal China. *J Antimicrob Chemother.* 2021;76:322–9.
17. Wang Y, Liu F, Zhu B, Gao GF. Discovery of tigecycline resistance genes *tet(X3)* and *tet(X4)* in live poultry market worker gut microbiomes and the surrounded environment. *Sci Bull.* 2020;65:340–2.
18. Guh AY, Bulens SN, Mu Y, Jacob JT, Reno J, Scott J, et al. Epidemiology of carbapenem-resistant enterobacteriaceae in 7 US communities, 2012–2013. *JAMA.* 2015;314:1479.
19. Zhang R, Liu L, Zhou H, Chan EW, Li J, Fang Y, et al. Nationwide surveillance of Clinical Carbapenem-resistant Enterobacteriaceae (CRE) strains in China. *EBioMedicine.* 2017;19:98–106.
20. Yong D, Toleman MA, Giske CG, Cho HS, Sundman K, Lee K, et al. Characterization of a new metallo-beta-lactamase gene, *bla_{NDM-1v}*, and a novel erythromycin esterase gene carried on a unique genetic structure in *Klebsiella pneumoniae* sequence type 14 from India. *Antimicrob Agents Chemother.* 2009;53:5046–54.
21. Han JW, Koh HB, Kim TJ. Molecular characterization of beta-lactamase-producing *Escherichia coli* collected from 2001 to 2011 from Pigs in Korea. *Foodborne Pathog Dis.* 2016;13:68–76.
22. Wang Y, Wu C, Zhang Q, Qi J, Liu H, Wang Y, et al. Identification of New Delhi metallo-beta-lactamase 1 in *Acinetobacter lwoffii* of food animal origin. *PLoS One.* 2012;7:e37152.
23. Li J, Bi Z, Ma S, Chen B, Cai C, He J, et al. Inter-host transmission of carbapenemase-producing *Escherichia coli* among humans and backyard animals. *Environ Health Perspect.* 2019;127:107009.
24. Li R, Liu Z, Li Y, Xiao X, Wang Z. Characterization of *bla_{NDM-1}*-positive enterobacteriaceae reveals the clonal dissemination of *Enterobacter hormaechei* coharboring *bla_{NDM-1}* and *tet(X4)* along the pork production chain. *Int J Food Microbiol.* 2022;372:109692.
25. Wang Y, Zhang R, Li J, Wu Z, Yin W, Schwarz S, et al. Comprehensive resistome analysis reveals the prevalence of NDM and MCR-1 in Chinese poultry production. *Nat Microbiol.* 2017;2:16260.
26. Dadashi M, Yaslianifard S, Hajikhani B, Kabir K, Owlia P, Goudarzi M, et al. Frequency distribution, genotypes and prevalent sequence types of New Delhi metallo-beta-lactamase-producing *Escherichia coli* among clinical isolates around the world: a review. *J Glob Antimicrob Resist.* 2019;19:284–93.
27. Huang Z, Li Y, Cai C, Dong N. Isolation, molecular characterization, and antimicrobial resistance of selected culturable bacteria from crayfish (*Procambarus clarkii*). *Front Microbiol.* 2022;13:911777.
28. Zhao Q, Zhu J, Cai R, Zheng X, Zhang L, Chang M, et al. IS26 is responsible for the evolution and transmission of *bla_{NDM-1}*-harboring plasmids in *Escherichia coli* of poultry origin in China. *mSystems.* 2021;6:e0064621.
29. Shen Z, Hu Y, Sun Q, Hu F, Zhou H, Shu L, et al. Emerging carriage of NDM-5 and MCR-1 in *Escherichia coli* from healthy people in multiple Regions in China: a cross sectional observational study. *EClinicalMedicine.* 2018;6:11–20.
30. Berrazeg M, Diene S, Medjahed L, Parola P, Drissi M, Raoult D, et al. New Delhi metallo-beta-lactamase around the world: an eReview using google maps. *Euro Surveill.* 2014;19:20809.
31. Kazmierczak KM, Rabine S, Hackel M, McLaughlin RE, Biedenbach DJ, Bouchillon SK, et al. Multiyear, multinational survey of the incidence and global distribution of metallo-beta-lactamase-producing enterobacteriaceae and *Pseudomonas aeruginosa*. *Antimicrob Agents Chemother.* 2016;60:1067–78.
32. Isozumi R, Yoshimatsu K, Yamashiro T, Hasebe F, Nguyen BM, Ngo TC, et al. *bla_{NDM-1}*-positive *Klebsiella pneumoniae* from environment, Vietnam. *Emerg Infect Dis.* 2012;18:1383–5.
33. Wang Y, Hu Y, Cao J, Bi Y, Lv N, Liu F, et al. Antibiotic resistance gene reservoir in live poultry markets. *J Infect.* 2019;78:445–53.
34. Wang Y, Hu Y, Cao J, Bi Y, Lv N, Liu F, et al. More diversified antibiotic resistance genes in chickens and workers of the live poultry markets. *Environ Int.* 2021;153:106534.
35. Tada T, Miyoshi-Akiyama T, Shimada K, Kirikae T. Biochemical analysis of metallo-beta-lactamase NDM-3 from a multidrug-resistant *Escherichia coli* strain isolated in Japan. *Antimicrob Agents Chemother.* 2014;58:3538–40.
36. Rahman M, Shukla SK, Prasad KN, Ovejero CM, Pati BK, Tripathi A, et al. Prevalence and molecular characterisation of New Delhi metallo-beta-lactamases NDM-1, NDM-5, NDM-6 and NDM-7 in multidrug-resistant Enterobacteriaceae from India. *Int J Antimicrob Agents.* 2014;44:30–7.
37. Makena A, Brem J, Pfeffer I, Geffen RE, Wilkins SE, Tarhonskaya H, et al. Biochemical characterization of New Delhi metallo-beta-lactamase variants reveals differences in protein stability. *J Antimicrob Chemother.* 2015;70:463–9.
38. Ntshobeni NB, Allam M, Ismail A, Amoako DG, Essack SY, Chenia HY, et al. Draft genome sequence of *Providencia rettgeri* APW139_S1, an NDM-18-producing clinical strain originating from hospital effluent in South Africa. *Microbiol Resour Annot.* 2019;8:e00259–e319.
39. Gao Y, Du P, Zhang P, Wang J, Liu Z, Fanning S, et al. Dynamic evolution and transmission of a *bla_{NDM-1}*-bearing fusion plasmid in a clinical *Escherichia coli*. *Microbiol Res.* 2023;275:127450.
40. Camargo CH, Yamada AY, Souza AR, Reis AD, Santos MBN, Assis DB, et al. Genomic diversity of NDM-producing *Klebsiella* species from Brazil, 2013–2022. *Antibiotics (Basel).* 2022;11:1395.
41. Humphries R, Bobenchik AM, Hindler JA, Schuetz AN. Overview of changes to the clinical and laboratory standards Institute performance standards for antimicrobial susceptibility testing, M100, 31st edition. *J Clin Microbiol.* 2021;59:e0021321.
42. Yin Y, Qiu L, Wang G, Guo Z, Wang Z, Qiu J, et al. Emergence and transmission of plasmid-mediated mobile colistin resistance gene *mcr-10* in humans and companion animals. *Microbiol Spectr.* 2022:e02097–22.
43. Bolger AM, Lohse M, Usadel B. Trimmomatic: a flexible trimmer for Illumina sequencing data. *Bioinformatics.* 2014;30:2114–20.
44. Bankevich A, Nurk S, Antipov D, Gurevich AA, Dvorkin M, Kulikov AS, et al. SPAdes: a new genome assembly algorithm and its applications to single-cell sequencing. *J Comput Biol.* 2012;19:455–77.
45. Ye L, Liu X, Ni Y, Xu Y, Zheng Z, Chen K, et al. Comprehensive genomic and plasmid characterization of multidrug-resistant bacterial strains by R10.4.1 nanopore sequencing. *Microbiol Res.* 2024;283:127666.
46. Wick RR, Judd LM, Gorrie CL, Holt KE. Unicycler: resolving bacterial genome assemblies from short and long sequencing reads. *PLoS Comput Biol.* 2017;13:e1005595.
47. Alikhan N-F, Petty NK, Ben Zakour NL, Beatson SA. BLAST Ring Image Generator (BRIG): simple prokaryote genome comparisons. *BMC Genomics.* 2011;12:402.
48. Sullivan MJ, Petty NK, Beatson SA. Easyfig: a genome comparison visualizer. *Bioinformatics.* 2011;27:1009–10.
49. Seemann T. Prokka: rapid prokaryotic genome annotation. *Bioinformatics.* 2014;30:2068–9.
50. Page AJ, Cummins CA, Hunt M, Wong VK, Reuter S, Holden MT, et al. Roary: rapid large-scale prokaryote pan genome analysis. *Bioinformatics.* 2015;31:3691–3.
51. Price MN, Dehal PS, Arkin AP. FastTree: computing large minimum evolution trees with profiles instead of a distance matrix. *Mol Biol Evol.* 2009;26:1641–50.
52. Clermont O, Christenson JK, Denamur E, Gordon DM. The Clermont *Escherichia coli* phylo-typing method revisited: improvement of specificity and detection of new phylo-groups. *Environ Microbiol Rep.* 2013;5:58–65.
53. Chen C, Chen H, Zhang Y, Thomas HR, Frank MH, He Y, et al. TBtools: an integrative toolkit developed for interactive analyses of big biological data. *Mol Plant.* 2020;13:1194–202.

Publisher's Note

Springer Nature remains neutral with regard to jurisdictional claims in published maps and institutional affiliations.